Role of Synaptic Filtering on the Firing Response of Simple Model Neurons

Rubén Moreno-Bote and Néstor Parga
Departamento de Física Teórica, Universidad Autónoma de Madrid, Cantoblanco, 28049 Madrid, Spain

(Received 5 June 2003; revised manuscript received 14 October 2003; published 15 January 2004)

During active states of the brain neurons process their afferent currents with an effective membrane time constant much shorter than its value at rest. This fact, together with the existence of several synaptic time scales, determines to which aspects of the input the neuron responds best. Here we present a solution to the response of a leaky integrate-and-fire neuron with synaptic filters when long synaptic times are present, and predict the firing rate for all values of the synaptic time constant. We also discuss under which conditions this neuron becomes a coincidence detector.

DOI: 10.1103/PhysRevLett.92.028102 PACS numbers: 87.19.La, 05.40.–a, 84.35.+i

Neurons process input currents originated from presynaptic spikes produced by many other neurons. One of the first processing steps is the synaptic filtering of the current with characteristic times τ_s which take a wide range of values that, for some synaptic types, can be quite long compared to the resting membrane time constant [1]. Long synaptic time constants also appear naturally in active states of the brain because the effective membrane time constant τ_m is significantly reduced due to the net increase in conductance resulting from background activity [2,3]. It is plausible that in these active states the effective membrane time constant becomes a dynamical variable that can operate in regimes where it is the shortest [3,4] as well as in regimes where it is an intermediate time scale [3]. Since synapses smooth current fluctuations, the precise relation between the effective membrane and synaptic time constants is specially relevant when the mean depolarization is below threshold, where the neuron response is mainly produced by current fluctuations. A quantitative description of the neuron response for any relation between the values of the synaptic and the effective membrane time constants is then desirable. Here we obtain the solution for the output firing rate of a model neuron driven by Poisson inputs presenting two important cases. In the first, τ_m is the shortest time scale. In the second, we deal with a very short synaptic time constant—an infinitely fast synapse—while all the other synaptic types have $\tau_s > \tau_m$. Using a procedure introduced in [5] we also show that an interpolation of the response between the short [6,7] and the long τ_s limits found here describes quite well the output firing rate of a leaky integrate-and-fire (LIF) neuron with synaptic filtering. Other work dealing with the effect of a single filter on the neural response can be found in [8,9]. However, in [8] an approximation valid in a rather restricted region of input parameters is used, while in [9] a different current statistics is considered.

The membrane potential V of the model neuron obeys

$$\tau_m \dot{V} = -V + \tau_m I(t), \tag{1}$$

where $I(t)$ is the total synaptic current. In the case of a single synaptic type it is

$$\tau_s \dot{I}(t) = -I(t) + J \sum_{i,k} \delta(t - t_i^k). \tag{2}$$

Here t_i^k labels the random time of the kth spike from the ith presynaptic neuron firing with Poisson statistics. J/τ_s is the size of the postsynaptic current generated by a single spike. A spike is evoked whenever V hits a threshold value Θ, from where it is reset to a hyperpolarized value, H.

In what follows we obtain the neuron response for two important situations: (i) there is only one slow synaptic type; (ii) τ_m lies between a single fast and a single slow filter. The most general cases where τ_m is intermediate between any number of fast and any number of slow filters can be derived from them. Specifically, when there are not fast filters, the neuron behaves as in (i), while if there is at least one fast filter, it behaves as in (ii).

(i) One slow synaptic type.—Since the number of presynaptic spikes is normally quite large and the evoked postsynaptic potentials are very small compared to the firing threshold, the spike train in Eq. (2) can be approximated [10] by its mean μ and variance σ^2 as

$$\tau_s \dot{I}(t) = -I(t) + \mu + \sigma \eta(t), \tag{3}$$

where $\eta(t)$ is a Gaussian white noise with zero mean and unit variance. The filter introduces exponential correlations in the current with a correlation time τ_s [6,11],

$$\langle (I(t) - \mu)(I(t') - \mu) \rangle = \frac{\sigma^2}{2\tau_s} e^{-(|t-t'|/\tau_s)}. \tag{4}$$

It is convenient to rewrite Eqs. (1) and (3) by performing the linear transformations $I = \mu + z\,\sigma/\sqrt{2\tau_s}$ and $V = \mu\tau_m + x\,\sigma\sqrt{\tau_m/2}$:

$$\dot{x} = -\frac{x}{\tau_m} + \frac{z}{\sqrt{\tau_m \tau_s}}, \tag{5}$$

$$\dot{z} = -\frac{z}{\tau_s} + \sqrt{\frac{2}{\tau_s}}\eta(t). \tag{6}$$

Note that the average of $z^2\sigma^2/2\tau_s$ gives the current fluctuations. In these units the threshold and reset potentials read $\hat{\Theta} = \sqrt{2}(\Theta - \mu\tau_m)/\sigma\sqrt{\tau_m}$ and $\hat{H} = \sqrt{2}(H - \mu\tau_m)/\sigma\sqrt{\tau_m}$. The stationary Fokker-Planck equation (FPE) [12] associated with Eqs. (5) and (6) is

$$\left[\frac{\partial}{\partial x}(x - \epsilon z) + \epsilon^2 L_z\right]P(x, z) = -\tau_m J(z)\delta(x - \hat{H}), \tag{7}$$

where $\epsilon = \sqrt{\tau_m/\tau_s}$ and $L_z = (\partial/\partial z)z + (\partial^2/\partial^2 z)$. $P(x, z)$ is the stationary probability density of having the neuron in the state (x, z). The source current $J(z)$ accounts for the reset effect: the flow of probability escaping at the threshold is reinjected at the reset potential with the same rate and distribution in z that it had when it escaped. $J(z)$ has to be determined in a self-consistent way, that is, it has to match the escaping current of the LIF neuron, which is the x component of the probability current vector evaluated at threshold. The equation relating $J(z)$ and $P(x, z)$ is obtained by writing Eq. (7) as the divergence of a probability current vector $\vec{J}(x, z)$ [12]. One easily finds that its x-axis component is $\tau_m J_x(x, z) = (-x + \epsilon z)P(x, z)$, which after setting $x = \hat{\Theta}$ yields

$$J(z) = \frac{1}{\tau_m}(-\hat{\Theta} + \epsilon z)P(\hat{\Theta}, z). \tag{8}$$

The output firing rate is then computed as ($z_{\min} = \hat{\Theta}/\epsilon$)

$$\nu_{\text{out}} = \int_{z_{\min}}^{\infty} dz J(z). \tag{9}$$

The escape current $J(z)$ is zero below $z_{\min}$ because there cannot be flow of probability from above $\hat{\Theta}$. Equations (7) and (8) have to be solved with appropriate boundary conditions. It is readily checked that a perturbative expansion of $P(x, z)$ and $J(z)$ in powers of ϵ is not defined in the subthreshold regime, although it works well if the mean depolarization $\mu\tau_m$ is above threshold. Below threshold the firing of the neuron is mainly controlled by the fluctuations, but since the filter smooths these fluctuations, they become quite weak for long τ_s. In fact, one can see from Eq. (5) that the fluctuations of the membrane potential are of the order of ϵ^2. This suggests a procedure to regularize the equations: one should first keep the membrane fluctuations finite and only at the end, after the regular part of the problem has been dealt with in a perturbative fashion, one can safely give them their correct value. This idea is implemented by replacing Eq. (5) by

$$\dot{x} = \frac{1}{\tau_m}(-x + \gamma z), \tag{10}$$

and setting the lower integration limit in Eq. (9) to $z_{\min} = \hat{\Theta}/\gamma$. Equation (6) is left unchanged. This procedure alters only slightly the system of Eqs. (7) and (8): the terms where $\epsilon z P(x, z)$ appears become $\gamma z P(x, z)$.

The perturbative expansion in powers of ϵ is now done at fixed γ. Only at the end of the calculation γ is given its correct value $\gamma = \epsilon = \sqrt{\tau_m/\tau_s}$. To proceed with the expansion we write

$$P = P_0 + \epsilon^2 P_1 + \ldots, \qquad J = J_0 + \epsilon^2 J_1 + \ldots, \tag{11}$$

and replace these expressions in Eqs. (7) and (8) (with γz in the place of ϵz, as we just said). We have now to impose order by order the conditions

$$P_n(\hat{\Theta}, z) = 0 \qquad \forall z < \hat{\Theta}/\gamma, \tag{12}$$

$$J_n(z) = \tau_m^{-1}(\gamma z - \hat{\Theta})P_n(\hat{\Theta}, z), \tag{13}$$

$$\int_{-\infty}^{\hat{\Theta}} dx \int_{-\infty}^{\infty} dz\, P_n(x, z) = \delta_{n,0}, \tag{14}$$

$$\lim_{z\to\pm\infty} z P_n \to 0, \qquad \lim_{x\to-\infty} x P_n \to 0, \tag{15}$$

where $\delta_{n,0} = 1$ for $n = 0$ and it is 0 otherwise. Integrating Eq. (7) over x and using Eqs. (12)–(15), we obtain the useful constraint

$$\int_{-\infty}^{\hat{\Theta}} dx P_n(x, z) = \delta_{n,0}\frac{e^{-z^2/2}}{\sqrt{2\pi}}, \tag{16}$$

which says that the marginal distribution of z has to be a normalized Gaussian. It is immediate to show that

$$\frac{\partial}{\partial x}(x - \gamma z)P_n + L_z P_{n-1} + \tau_m J_n(z)\delta(x - \hat{H}) = 0, \tag{17}$$

with $P_{-1} = 0$. We are interested in the leading order, thus by solving the equation for $n = 0$ we have

$$P_0(x, z) = \frac{\tau_m J_0(z)\mathcal{H}(x - \hat{H})}{\gamma z - x} + D(z)\delta(x - \gamma z)\mathcal{H}(\hat{\Theta}/\gamma - z), \tag{18}$$

where $D(z)$ depends only on z. $\mathcal{H}(t) = 1$ when $t > 0$ and it is zero otherwise. Replacing P_0 into the constraint (16) gives $D(z) = e^{-z^2/2}/\sqrt{2\pi}$ and

$$J_0(z) = \frac{e^{-z^2/2}}{\sqrt{2\pi}}\,\mathcal{F}_0(\hat{H} - \gamma z, \hat{\Theta} - \gamma z), \tag{19}$$

where we have defined $\mathcal{F}_0^{-1}(a, b) = \tau_m \log(a/b)$. At this step we proceed to replace γ by $\epsilon = \sqrt{\tau_m/\tau_s}$. Introducing $J_0(z)$ into Eq. (9) leads to the following formula for the output firing rate at zeroth order:

$$\nu_{\text{out}} = \int_{\hat{\Theta}/\epsilon}^{\infty} \frac{dz}{\sqrt{2\pi}}\, e^{-z^2/2}\, \mathcal{F}_0(\hat{H} - \epsilon z, \hat{\Theta} - \epsilon z). \tag{20}$$

This remarkable result has a clear intuitive meaning. In the $\tau_s \to \infty$ limit, the variable z changes very little for a time τ_m. It can then be assumed that the neuron experiences a drift $-x + \epsilon z$ with constant z. At fixed z, $\mathcal{F}_0(\hat{H} - \epsilon z, \hat{\Theta} - \epsilon z)$ is the firing rate of a LIF neuron driven by a noiseless effective current $I_{\rm eff} = \mu + z\sigma/\sqrt{2\tau_s}$ [10]. Because the stationary distribution of z is Gaussian with unit variance, and because the current at the threshold has to be positive, Eq. (20) is readily obtained by averaging $\mathcal{F}_0(\hat{H} - \epsilon z, \hat{\Theta} - \epsilon z)$ over z.

It is also remarkable that Eq. (20) does not admit an expansion in powers of τ_s^{-1} in the full space of input parameters. In the *subthreshold regime* ($\hat{\Theta} > 0$) the expansion is not defined, as can be seen by evaluating the function and its derivatives at long τ_s. Because the neuron fires only if $z > z_{\rm min}$ and because, for long τ_s, $z_{\rm min}$ takes a value close to 1 standard deviation of the Gaussian distribution of z, the neuron fires only when low probability fluctuations occur. It is concluded that, in the subthreshold regime, the neuron behaves as a *coincidence detector* instead of as a simple integrator. Figure 1 illustrates this behavior as τ_s becomes long: only when large, rare fluctuations occur ($z > z_{\rm min}$), the membrane potential can reach the threshold and produce spikes. When such a fluctuation occurs, it remains present for a time τ_s and, if it is big enough, the neuron emits a burst of spikes, leading to high output variability.

In the *suprathreshold regime* the expansion does exist. Up to order $O(\tau_s^{-1})$, the output rate is

$$\nu_{\rm out} \sim \tilde{\nu}_0 + \frac{C_1}{\tau_s}, \qquad C_1 = \tau_m^2 \tilde{\nu}_0^2 \left[\tau_m \tilde{\nu}_0 (\hat{\Theta}^{-1} - \hat{H}^{-1})^2 - \frac{\hat{\Theta}^{-2} - \hat{H}^{-2}}{2} \right], \tag{21}$$

where $\tilde{\nu}_0 = \mathcal{F}_0(\hat{H}, \hat{\Theta})$. Equation (21) takes into account all the corrections to the output rate at order τ_s^{-1}. In this regime the neuron behaves as an *integrator*, because its firing is mainly driven by the mean input current [see Eq. (21)], and it is not very sensitive to synaptic fluctuations. This coding mechanism clearly contrasts with that employed by the neuron in the subthreshold regime.

(ii) One fast and one slow synaptic types.—In a scenario where the effective membrane time constant τ_m changes dynamically, it can take values of a few milliseconds, intermediate between the synaptic time constants of one short and one long synaptic type. This is the case found in a recent study [3] about the effect of background activity on τ_m when excitatory AMPA (fast) and inhibitory GABA (slow) [1] synaptic receptors are present. In this case the total current has two contributions, $I(t) = I_1(t) + I_2(t)$, which in the diffusion limit are

$$\tau_s \dot{I}_1(t) = -I_1(t) + \mu_1 + \sigma_1 \eta(t), \qquad I_2(t) = \mu_2 + \sigma_2 \zeta(t). \tag{22}$$

The quantities μ_1, μ_2, and σ_1^2, σ_2^2 are the means and variances of the inhibitory and excitatory currents, and $\eta(t)$ and $\zeta(t)$ are two independent white noise processes with unit variance. Defining $\mu \equiv \mu_1 + \mu_2$ and performing the linear transformation $I_1 = \mu_1 + z\sigma_1/\sqrt{2\tau_s}$ and $V = \mu\tau_m + x\sigma_2\sqrt{\tau_m/2}$, the equation for z is still Eq. (6), but now x obeys

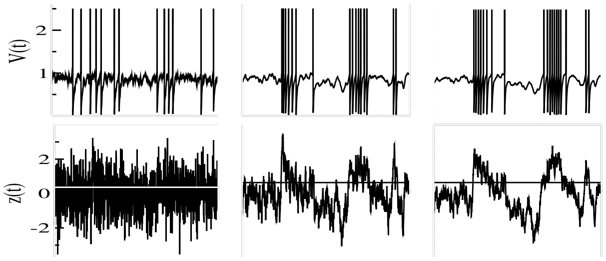

FIG. 1. Membrane potential $V(t)$ (top) and $z(t)$ (bottom) during 1.4 s for one synaptic type with $\tau_s = 1$, 20, and 50 ms, from left to right. The straight lines in the bottom plots represent $z_{\rm min} = \hat{\Theta}/\epsilon$. Parameters have been chosen to produce in all cases approximately the same firing rates (~12 Hz) and are $\tau_m = 10$ ms, $\Theta = 1$, and $H = 0$ (in arbitrary units), $\mu = 80\ {\rm s}^{-1}$, and $\sigma^2 = 1.5$, 10, and 25 ${\rm s}^{-1}$ from left to right ($z_{\rm min} = 0.63$ in the last two cases). The coefficients of variation of the interspike intervals are, from left to right, 0.7, 1.1, and 1.5.

$$\dot{x} = \frac{1}{\tau_m}[-x + \sqrt{2\tau_m}\zeta(t) + \sqrt{\alpha}\gamma\, z] \tag{23}$$

instead of Eq. (10). Again we write γ in place of ϵ. Here $\alpha \equiv \sigma_1^2/\sigma_2^2$, and the threshold and reset potentials now become $\hat{\Theta} = \sqrt{2}(\Theta - \mu\tau_m)/\sigma_2\sqrt{\tau_m}$ and $\hat{H} = \sqrt{2}(H - \mu\tau_m)/\sigma_2\sqrt{\tau_m}$. The current autocorrelation is

$$\langle (I(t) - \mu)(I(t') - \mu) \rangle = \sigma_2^2 \delta(t - t') + \frac{\sigma_1^2}{2\tau_s} e^{-(|t-t'|/\tau_s)} \tag{24}$$

and the stationary FPE reads

$$\left[L_x - \gamma\sqrt{\alpha} z \frac{\partial}{\partial x} + \epsilon^2 L_z \right] P(x, z) = -\tau_m J(z) \delta(x - \hat{H}). \tag{25}$$

The escape current can be obtained from here in a self-consistent way (see [5,12]). The perturbative calculation proceeds as in the case of a single filter (in particular γ is kept fixed until the end). Now condition (12) becomes $P_n(\hat{\Theta}, z) = 0$ for all n. The output firing rate is

$$\nu_{\rm out} = \int_{-\infty}^{\infty} \frac{dz}{\sqrt{2\pi}}\, e^{-(z^2/2)} \mathcal{F}(\hat{H} - \epsilon\sqrt{\alpha} z, \hat{\Theta} - \epsilon\sqrt{\alpha} z), \tag{26}$$

where we have defined the quantities $\mathcal{F}^{-1}(a, b) = \tau_m \int_a^b dt\, R(t/\sqrt{2})$ and $R(t) = \sqrt{\pi/2}\, e^{t^2}[1 + {\rm erf}(t)]$, and ${\rm erf}(t)$ is the error function. The quantity $\mathcal{F}$ in Eq. (26) has also an intuitive meaning: it is the rate of a LIF neuron driven by a current with effective mean $\mu_{\rm eff} = \mu + z\sigma_1/\sqrt{2\tau_s}$ and variance σ_2^2 [10]. For vanishing σ_2, Eq. (26) converges to the previous result, Eq. (20). The output firing rate obtained by expanding Eq. (26) up to $O(\epsilon^2)$ is

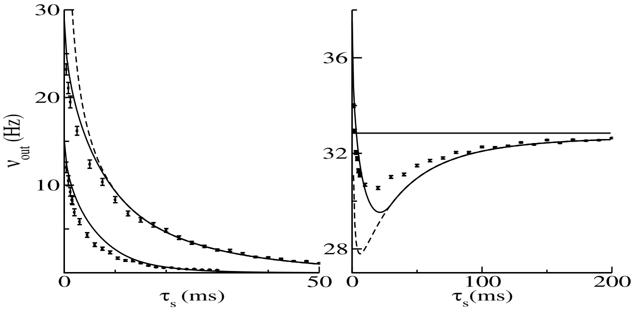

FIG. 2. Output firing rate as a function of τ_s in the sub- and the suprathreshold regimes. Left: Subthreshold regime with $\mu = 80\ \mathrm{s}^{-1}$, and $\sigma^2 = 12\ \mathrm{s}^{-1}$ (upper curve), $\sigma^2 = 4\ \mathrm{s}^{-1}$ (bottom curve). Full lines: predicted rate using the interpolation procedure with $\tau_{s,\mathrm{inter}} = 15$ ms. Right: Suprathreshold regime with $\mu = 105\ \mathrm{s}^{-1}$, and $\sigma^2 = 1\ \mathrm{s}^{-1}$. Full line: predicted rate with $\tau_{s,\mathrm{inter}} = 30$ ms. Straight line: infinite τ_s limit. In all cases, $\tau_m = 10$ ms, $\Theta = 1$, and $H = 0$ (in arbitrary units), the data points are the corresponding simulation results and the dashed lines are the long τ_s predictions, Eq. (20).

$$\nu_{\mathrm{out}} = \nu_0 + \frac{C_2}{\tau_s},$$
$$C_2 \equiv \alpha \tau_m^2 \nu_0^2 \bigg[\tau_m \nu_0 [R(\hat{\Theta}/\sqrt{2}) - R(\hat{H}/\sqrt{2})]^2 - \frac{\hat{\Theta} R(\hat{\Theta}/\sqrt{2}) - \hat{H} R(\hat{H}/\sqrt{2})}{2} \bigg]. \tag{27}$$

In the presence of fast noise the neuron is an integrator in both the supra- and the subthreshold regimes. Firing is mainly due to the mean current μ and the fast noise σ_2. This is seen in that the leading term in Eq. (27), $\nu_0 = \mathcal{F}(\hat{H}, \hat{\Theta})$, is the rate of a standard integrator [10] receiving a current with these characteristics. That rare fluctuations are not relevant can be seen from the fact that this leading term comes from $z = 0$ in Eq. (26).

Interpolating between the short and long τ_s limits.— For a single filter it is possible to obtain a good prediction of the response of the neuron for any value of the ratio τ_m/τ_s. The effect of a single filter with a short τ_s on the rate for crossing an absorbing barrier was studied in [11], where it was shown to be of order $\sqrt{\tau_s}$. A similar technique was used to compute the response of a LIF neuron [6,7] obtaining

$$\nu_{\mathrm{out}} = \tilde{\nu}_0 - 1.46\, \sqrt{\tau_s \tau_m}\, \tilde{\nu}_0^2 \bigg[R\Big(\frac{\hat{\Theta}}{\sqrt{2}}\Big) - R\Big(\frac{\hat{H}}{\sqrt{2}}\Big) \bigg]. \tag{28}$$

We can now interpolate between the two limits, Eqs. (20) and (28), by introducing additional dependencies of the firing rate on τ_s, following a procedure introduced in [5]. At short τ_s we use $\nu_{\mathrm{out}} = \tilde{\nu}_0 + A\sqrt{\tau_s} + B\tau_s + C\tau_s^{3/2}$, where A is the coefficient of the correction term in Eq. (28), while at long τ_s we employ Eq. (20). Both limits are joined at $\tau_{s,\mathrm{inter}} \sim \tau_m$, and B and C are set to obtain a continuous and derivable interpolating curve at $\tau_s = \tau_{s,\mathrm{inter}}$.

We have tested our results and the interpolation procedure generating random walk samples from the stochastic equations (5) and (6). Figure 2 shows the neuron response as a function of τ_s. Notice that while in the subthreshold regime (left) the rate decreases monotonically as τ_s, in the suprathreshold regime (right) it has a minimum. The prediction is rather accurate and, remarkably, it is close to the true rate even for $\tau_s \sim \tau_m$.

The interpolation can be also done for τ_m intermediate between a fast and a slow filter. If α is small the procedure is exactly the same employed in [5]. This is because the current correlations induced by two synaptic types, Eq. (24), can be interpreted as correlations in the presynaptic spike trains themselves [5] (α has to be reinterpreted as the correlation amplitude). The output rate at long τ_s given in Eq. (26) improves the results presented in [5] because the present treatment does not impose any restriction on the value of α.

We have found that a LIF neuron with only slow synaptic filters acts as a detector of rare synaptic fluctuations, Eq. (20). But how can these fluctuations be generated? These are produced when there are coincidences in the arrival times of a large number of spikes with a temporal precision τ_s. When the inputs are synchronized, rare fluctuations are generated in the same way, but coincidences and thus large fluctuations are now more likely (this can be considered in our formalism by renormalizing σ in Eq. (20) (see [5]). While with only slow filtering a neuron acts as a coincidence detector, the presence of a fast filter (even with finite short $\tau_s < \tau_m$) prevents the neuron from behaving in this way, and the response looks similar to the first graph in Fig. 1. These results show that the interplay between membrane and synaptic time constants is crucial for determining the neuronal behavior and give a quantitative description of the phenomenon.

[1] M. F. Bear, B.W. Connors, and M. A. Paradiso, *Neuroscience: Exploring the Brain* (Wiliams & Wilkins, Baltimore, Maryland, 1996).
[2] Ö. Bernander, R. J. Douglas, K. A. Martin, and C. Koch, Proc. Natl. Acad. Sci. U.S.A. **88**, 11 569 (1991).
[3] A. Destexhe, M. Rudolph, J. M. Fellous, and T. J. Sejnowski, Neuroscience **107**, 13 (2001).
[4] M. Shelley, D. McLaughlin, R. Shapley, and D. J. Wielaard, J. Comput. Neurosci. **13**, 93 (2002).
[5] R. Moreno, J. de la Rocha, A. Renart, and N. Parga, Phys. Rev. Lett. **89**, 288101 (2002).
[6] N. Brunel and S. Sergi, J. Theor. Biol. **195**, 87 (1998).
[7] N. Fourcaud and N. Brunel, Neural Comput. **14**, 2057 (2002).
[8] G. Svirskis and J. Rinzel, Biophys. J. **79**, 629 (2000).
[9] E. Salinas and T. J. Sejnowski, Neural Comput. **14**, 2111 (2002).
[10] L. M. Ricciardi, *Diffusion Processes and Related Topics in Biology* (Springer-Verlag, Berlin, 1977).
[11] C. R. Doering, P. S. Hagan, and C. D. Levermore, Phys. Rev. Lett. **59**, 2129 (1987).
[12] H. Risken, *The Fokker-Planck Equation* (Springer-Verlag, Berlin, 1989), 2nd ed.